

Characterization of Waste from the Dicalcium Phosphate Industry as a Potential Secondary Source of Rare Earth Elements [†]

Marcin Płachciak ^{1,*}, Fidel Grandia ¹ , Vladimir Roddatis ²  and Marcin Daniel Syczewski ²

¹ Amphos21 Consulting S.L., Carrer de Venèçuela 103 2° 1a, 08019 Barcelona, Spain; fidel.grandia@amphos21.com

² PISA Facility, Helmholtz Zentrum Potsdam Deutsches GeoForschungsZentrum-GFZ, Telegrafenberg, 14473 Potsdam, Germany; vladimir.roddatis@gfz-potsdam.de (V.R.); marcin.syczewski@gfz-potsdam.de (M.D.S.)

* Correspondence: marcin.plachciak@amphos21.com; Tel.: +34-644005326

[†] Presented at the 2nd International Conference on Raw Materials and Circular Economy “RawMat2023”, Athens, Greece, 28 August–2 September 2023.

Abstract: Fluorite-rich sludge is the main waste from dicalcium phosphate (DCP) production. This sludge consists of 40–60% of CaF₂, which precipitates during the reaction between fluorapatite (the main component of raw phosphorite material) and HCl. In addition, the sludge contains elevated amounts of critical elements such as REEs. In this study, two industrial sites producing DCP in Spain were studied to assess the potential valorization of these sludges. Currently, almost 2 Mt of waste remains landfilled in these sites. The concentrations of Y, La, Nd, Dy, and Gd found within the residues are about 1100 ppm, 450 ppm, 300 ppm, 80 ppm, and 75 ppm, respectively. Fluorite, being the host mineral of the REEs, occurs as very fine-grained spherules (<5 μm) that are smaller than other minerals in the waste (quartz, gypsum), favoring the options of hydrometallurgical separation. REEs extraction from the fluorite could be an advantageous option, if separated from uranium, which is the main environmental concern of the future valorization of this kind of waste.

Keywords: fluorite sludge; REE; recycling



Citation: Płachciak, M.; Grandia, F.; Roddatis, V.; Syczewski, M.D.

Characterization of Waste from the Dicalcium Phosphate Industry as a Potential Secondary Source of Rare Earth Elements. *Mater. Proc.* **2023**, *15*, 34. <https://doi.org/10.3390/materproc2023015034>

Academic Editors: Antonios Peppas, Christos Roumpos, Charalampos Vasilatos and Anthimos Xenidis

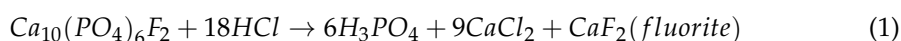
Published: 6 November 2023



Copyright: © 2023 by the authors. Licensee MDPI, Basel, Switzerland. This article is an open access article distributed under the terms and conditions of the Creative Commons Attribution (CC BY) license (<https://creativecommons.org/licenses/by/4.0/>).

1. Introduction

Dicalcium phosphate (DCP) is produced worldwide mostly for its use as an additive for animal feed in chicken farming [1]. In Spain, this good has been manufactured using sedimentary phosphate rocks (or phosphorites) from North Africa (mostly Morocco) [2]. These phosphorites (occurring as fluorapatite or francolite) are characterized by significant concentrations of Rare Earth Elements (REEs). The most common methods used to obtain phosphoric acid are the reaction of fluorapatite with H₂SO₄ or HCl (reaction 1). A sulfuric acid path is usually used for the manufacture of fertilizers, producing a waste called phosphogypsum, while a hydrochloric acid path is used for DCP production, generating a waste called fluorite sludge [3,4]. Subsequently, phosphoric acid is treated with limestone and results in the production of DCP, according to reaction 2 [4].



The reaction of phosphate rock with HCl triggers the precipitation of fluorite (also called fluorspar), as well as some accessory minerals such as quartz and gypsum, depending on the mineral impurities from the raw material. The precipitation of fluorite is relevant from the point of view of the trace elements originally occurring in the phosphorites; this

raw material may contain considerable concentrations of REEs as well as radionuclides from the ^{238}U and ^{232}Th series, which are subsequently fractionated mainly into the fluorite sludge; these radioactive elements cause this residue to be considered as a Naturally Occurring Radioactive Material (NORM) [2]. The phosphoric acid manufactured during the reaction does not incorporate significant amounts of REEs (the concentrations vary from a few ppb to a few hundred ppb). It is worth mentioning that phosphogypsum also contains elevated concentrations of REEs due the use of the same raw material, but these concentrations are not so high as in the case of fluorite sludge [3].

The residues generated during the production of phosphoric acid are generally stored in the landfills in the proximity of the factories. Considering the concentration of REEs that is present in the fluorite sludge and the substantial amount of the residues stored (around 2 Mt just in two sites in Spain; see below), they could constitute a potential secondary source of REEs. The objective of this study is to provide a thorough geochemical characterization of fluorite sludge to provide clues for further valorization at the industrial scale.

2. Case Studies

Two sites containing fluorite sludge stored in landfills were investigated in this study: (1) El Hondón-Cartagena in south Spain, which stopped production in 2001, and (2) Flix in NE Spain, where the manufacture of DCP is currently suspended. Both sites can be seen in Figure 1.

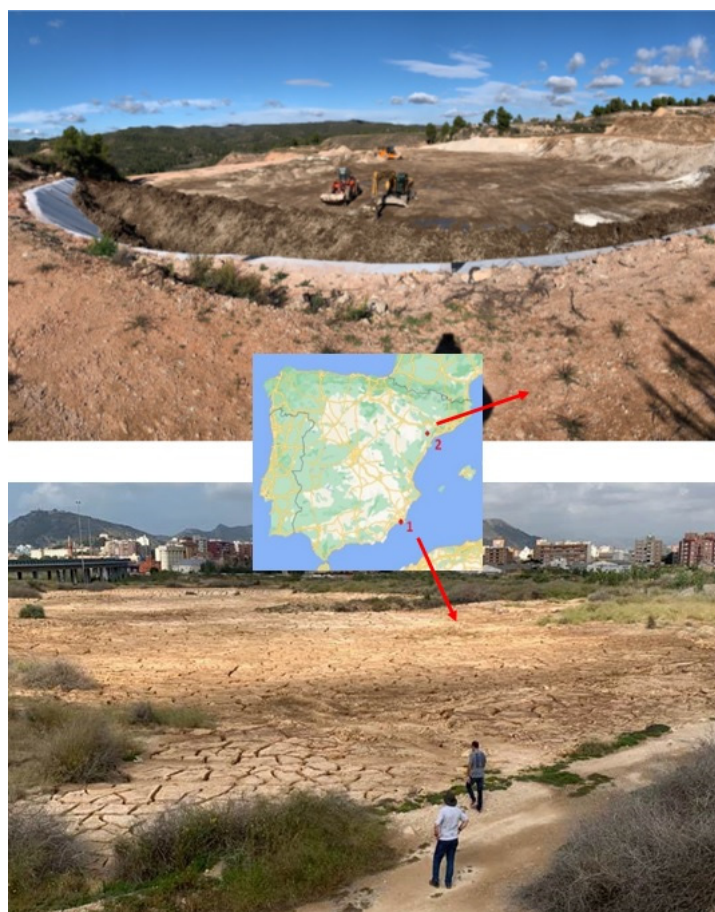


Figure 1. View of the fluorite sludge landfills and the locations of the studied sites in Spain: (1) El Hondón-Cartagena; (2) Flix.

2.1. El Hondón-Cartagena

The former industrial site of “El Hondón” is situated west of Cartagena in southern Spain (Murcia province) and produced DCP for almost 50 years (from the 1950s to 2001) [5].

The production rate of fluorite sludge was several tenths of thousands of tons per year, accumulating around 1 Mt in total, which was disposed in ponds and stockpiles on a landfill, covering a total area of around 108 ha. Different types of waste were accumulated in El Hondón: fluorite sludges, pyrite ashes and demolition material. The site is currently pending to be restored to minimize the environmental and radiological impacts, and a restoration plan has already been presented to the regional authorities.

2.2. Flix

The industrial plant in Flix in Catalonia in NE Spain has been producing DCP with a rate of 100 kt per year (50 kt of residues) since 1973 until its temporary shutdown in January 2023 [5]. Since the onset of the production until 1987, all of the waste originated from the Flix factory were disposed into the nearby reservoir [2]. After 1987, the manufacturer began to separate the solids from the process water, which was subsequently purified, and dumped both in a disposal area in the proximity of the plant, accumulating approx. 1 Mt of fluorite sludge.

3. Materials and Methods

3.1. Sampling

Two sampling campaigns were carried out in March and September 2022 for both El Hondón and Flix, collecting solid samples from the sites. Figure 2 shows the location of sampling points in El Hondón. Additionally, a raw phosphorite sample, a fresh fluorite sludge sample and two sludge samples from each of the three decantation tanks were obtained from the Flix industrial complex. These tanks are used to store the sludges that have just precipitated through the reaction of the material with HCl before traveling to the final disposal site. It allows for an increase in the efficiency of the production of phosphoric acid and decreases the amount of untreated phosphorite.



Figure 2. Sampling locations of landfill in El Hondón. A1–A12: piles; B1–B6: ponds.

Waste samples were collected from the first tenths of centimeters from the surfaces of the landfills with a shovel and stored in polyethylene bags. Figure 3 illustrates soil samples collected from El Hondón site.



Figure 3. Waste samples collected from El Hondón site.

3.2. Sample Analysis

The collected samples were thoroughly characterized using a variety of techniques. The samples were shipped to Actlabs (Activation Laboratories) in Canada, where they were prepared using lithium metaborate/tetraborate fusion and analyzed using Inductively Coupled Plasma–Mass Spectrometry and Optical Emission Spectrometry (ICP-MS and ICP-OES) for the determination of the concentration of major and trace elements (including REEs); Ion Selective Electrode analysis (ISE) was used to determine the concentration of F. They were also analyzed for the distribution of particle sizes (only Flix samples), and X-ray Diffraction (XRD) was used for the determination of the mineralogy of the samples. The samples used for the particle size analysis were placed in the water before the analysis, while the samples used for XRD were disaggregated, dispersed and placed in the holder, orienting the minerals. Quantitative mineralogical analysis in XRD was obtained using the Rietveld method. Additionally, the samples were analyzed using a Scanning Electron Microscope (SEM) and Transmission Electron Microscope (TEM) by the PISA facility in Helmholtz Zentrum Potsdam Deutsches GeoForschungsZentrum, Germany for mineralogical characterization and REE elemental analysis. All SEM measurements were performed using a crossbeam FEI Quanta 3D scanning electron microscope operating at 20 kV. To measure the REEs content, energy dispersive spectrometry (Edax Octane Elect Plus) was used. The X-ray spectra were collected with 4, 16, and 48 nA with a time of acquisition from 30 to 500 s per spectra. A Thermo Fisher Scientific (TFS) Transmission Electron Microscope Themis Z was used to perform EDX studies of two types of TEM specimens. Finally, the samples were analyzed via μ X-ray Fluorescence (μ XRF) using LUCIA beamline at the SOLEIL synchrotron facility (under proposal number 2021173) for the determination of the host mineral phases of REEs inside of the residues. Treatment of the data acquired via the beamline was carried out using Pymca5.6.7 software [6]. μ XRF was performed using a 2 μ m beam size to generate 2D compositional maps. The maps at two different incident energies (4 and 7.8 keV) were obtained to follow the lines of the Ca, F and REEs and locate these elements. They were chosen due to the hypothesis that fluorite (CaF_2) hosts rare earths in the sludge.

4. Results and Discussion

4.1. ICP and ISE

4.1.1. Major Elements

The bulk chemical composition analysis was conducted via ICP-OES and ISE for F (Table 1). These results show that the fluorite sludge samples from Flix and El Hondón consist of Ca, F and Si, which occur in major phases from fluorite sludge. The high LOI could be associated with the evaporation of the porewater inside of the sludge and the dehydration of the gypsum, which was relatively abundant in the samples (see Section 4.3).

Table 1. Major composition (wt.%) of the fluorite sludge samples measured using ICP-OES and ISE (for F). FL: sample from Flix; EH: sample from El Hondón; b.d.l.: below detection limit.

Composition	FL	EH
F	18.70	16.70
SiO ₂	12.02	7.49
Al ₂ O ₃	1.38	2.20
Fe ₂ O ₃ (T)	0.78	1.13
MnO	0.01	b.d.l.
MgO	0.30	0.41
CaO	42.52	40.09
Na ₂ O	0.21	1.37
K ₂ O	0.14	0.39
TiO ₂	0.08	0.13
P ₂ O ₅	8.41	9.95
LOI	23.22	15.91
Total	89.07	79.06

4.1.2. Trace Elements, including REEs

The samples of the fluorite sludge show elevated concentrations of metals, such as Cr, V, Zn, Sr, Ba and Zr (Table 2). The actual compositions of these elements vary within the samples, depending on the origin; the sample from Flix was obtained directly from the plant, and the one from El Hondón was obtained from the landfill. Moreover, the El Hondón site is characterized by the presence of waste from other industrial activities on the site that explains the differences in the concentrations of some trace elements.

Table 2. Concentrations of trace elements (excluding REE, Y, Sc, Th and U) within the fluorite sludge samples (ppm). FL: sample from Flix; EH: sample from El Hondón, b.d.l.: below detection limit.

Element	FL	EH	Element	FL	EH
Be	2	2	Mo	15	14
V	262	582	Ag	6.3	b.d.l.
Cr	330	730	In	b.d.l.	b.d.l.
Co	b.d.l.	b.d.l.	Sn	b.d.l.	1
Ni	130	80	Sb	2.5	10.8
Cu	170	70	Cs	0.6	1.9
Zn	810	220	Ba	934	153
Ga	3	6	Bi	b.d.l.	b.d.l.
Ge	b.d.l.	b.d.l.	Hf	2.4	1.9
As	b.d.l.	22	Ta	0.6	1.3
Rb	7	13	W	4	4
Sr	880	313	Tl	0.2	b.d.l.
Zr	133	120	Pb	5	10
Nb	5	3			

An analysis of the samples using ICP-MS showed that all of the REEs, which were originally found in the raw phosphorite, were partitioned into the fluorite sludge. Their concentrations within the waste were significant, with the average values from the landfill in El Hondón of 1177 ppm for Y, 450 ppm for La, 333 ppm for Nd, 223 ppm for Ce and less than 100 ppm for the remaining REEs (Table 3). The sample from Flix was characterized by smaller concentrations of REEs with the values of 695 ppm, 334 ppm, 216 ppm and 150 ppm for Y, La, Nd and Ce, respectively with the concentrations of the other REEs being smaller than 70 ppm (Table 3). It is also worth noting that the value for U is approx. 230 ppm in the case of El Hondón and around 500 ppm in the case of the Flix samples (Table 3). Compared to phosphorite rock, some sludge samples show an increase of 300–400% for REEs and 300% for U (Figure 4).

Table 3. Concentrations of REEs, Y, Sc, Th and U in the fluorite sludge samples and phosphorite (ppm). A1–A12: solid fluorite sludge samples from the piles in El Hondón; B2–B5: fluorite sludge samples from the ponds in El Hondón; AVG EH: average concentration of the fluorite sludge from El Hondón; FL: fluorite sludge sample from Flix site; T1–T3: fluorite sludge from the decantation tanks from Flix site; PR: phosphorite; nd: no data. Some values of Y were determined by a laboratory with 1000 ppm as a higher detection limit.

Element	Sc	Y	La	Ce	Pr	Nd	Sm	Eu	Gd	Tb	Dy	Ho	Er	Tm	Yb	Lu	Th	U
A1_1	34	1176	484	188	73	318	65	17	85	14	95	22	68	9	63	11	19	299
A1_2	nd	1220	492	174	70	315	65	17	95	13	91	22	74	11	67	11	19	165
A1_3	nd	762	285	107	43	194	39	10	56	8	55	13	43	6	40	7	8	141
A3_1	31	1140	446	162	66	281	58	15	75	12	83	20	64	9	62	11	16	293
A3_2	nd	1435	577	219	85	382	78	20	109	15	107	26	83	12	77	13	21	287
A12	35	1209	495	198	75	324	67	18	87	13	95	22	70	10	66	12	21	253
B2_1	33	1169	471	195	73	315	66	17	84	13	92	22	70	10	66	12	23	249
B2_2	nd	1105	641	704	124	539	106	25	119	16	101	23	70	10	58	9	57	164
B3_1	35	1340	528	226	86	369	78	20	96	15	106	24	74	10	68	12	23	212
B3_2	nd	>1000	475	194	72	350	65	17	100	13	94	24	70	11	67	nd	18	210
B3_3	nd	>1000	464	203	82	320	63	20	107	13	100	23	71	10	68	nd	19	215
B3_4	nd	1250	507	181	73	332	67	18	98	14	94	23	73	11	67	11	17	245
B3_5	nd	1145	465	176	68	306	61	16	89	12	85	21	68	10	61	10	17	196
B4	nd	1320	526	220	76	346	70	18	103	14	96	24	75	11	68	12	21	294
B5	nd	1030	450	203	70	309	65	17	88	12	82	19	61	9	55	9	22	247
AVG EH	34	1177	487	223	76	333	68	18	93	13	92	22	69	10	64	11	21	231
FL	22	695	334	150	49	216	45	12	57	9	65	16	49	7	47	8	14	490
T1_1	nd	871	335	142	60	224	42	12	76	10	66	17	49	7	50	nd	12	309
T1_2	nd	817	318	132	48	226	46	13	67	8	58	15	47	7	47	nd	11	312
T2_1	nd	>1000	765	333	133	516	109	27	166	21	161	38	117	16	114	nd	28	400
T2_2	nd	>1000	816	341	123	616	109	27	167	22	152	38	116	19	118	nd	30	442
T3_1	nd	>1000	690	301	120	452	100	27	143	20	146	34	103	15	99	nd	25	428
T3_2	nd	>1000	697	313	120	472	98	26	158	20	147	33	109	14	108	nd	25	429
PR	nd	235	98	40	15	66	14	4	20	3	19	5	15	2	13	2	3	124

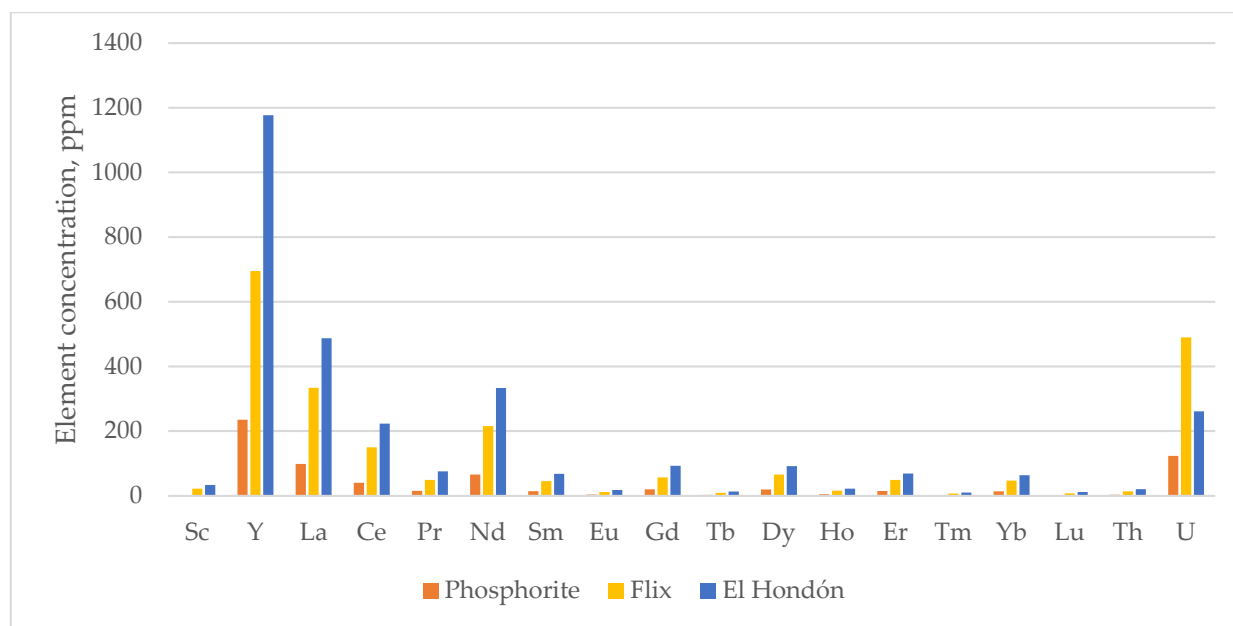


Figure 4. Concentrations of REEs, Sc, Y, Th and U in the phosphorite rock and fluorite sludge waste from Flix and El Hondón.

The samples from the decantation tanks show the highest concentrations of REEs among all of the samples, with values of up to 816 ppm, 616 ppm and 341 ppm for La, Nd and Ce, respectively. The enrichment of these samples compared to the fresh sludge from Flix is on the level of 120–190% (Figure 5). Due to the high quantities of REEs within the samples, fluorite sludge could potentially be considered as an important secondary source of REEs. The sludge from the landfills already presents a high potential for recycling, but the prior treatment of the sludge coming from the process directly from the decantation tanks instead of landfilling is an even more promising option. However, due to the significant activities of radionuclides inside of the samples (mainly uranium), their removal would have to be considered first.

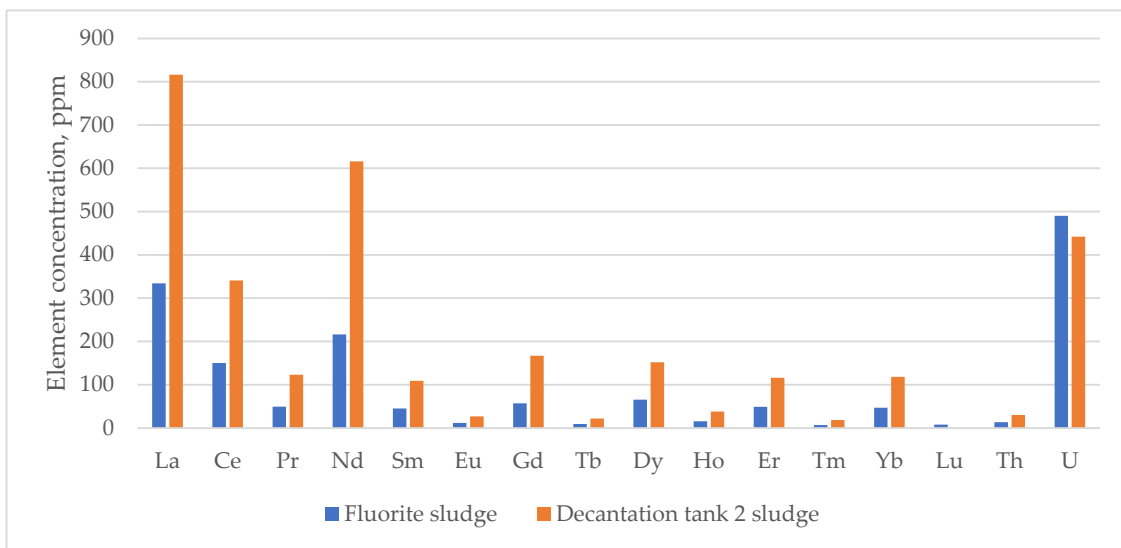


Figure 5. Concentrations of REEs, Th and U in the fluorite sludge sample and in the decantation tank 2 sludge sample from Flix industrial complex.

4.2. Particle Size Analysis

The analysis of the particle size distribution shows that the phases within the sludges are characterized by extremely small sizes, as can be seen in Figure 6. The diameter of all of the particles is smaller than 12 μm with a mean diameter 4.2 μm, while 65% of the particles have a diameter of less than 5 μm. Such small dimensions could provide some issues in the potential extraction of trace elements from the residue. It is worth noting that the particle size analysis was performed only for the samples coming from the landfill in Flix; hence, the mineralogy and sizes can be slightly distinct to the samples from El Hondón.

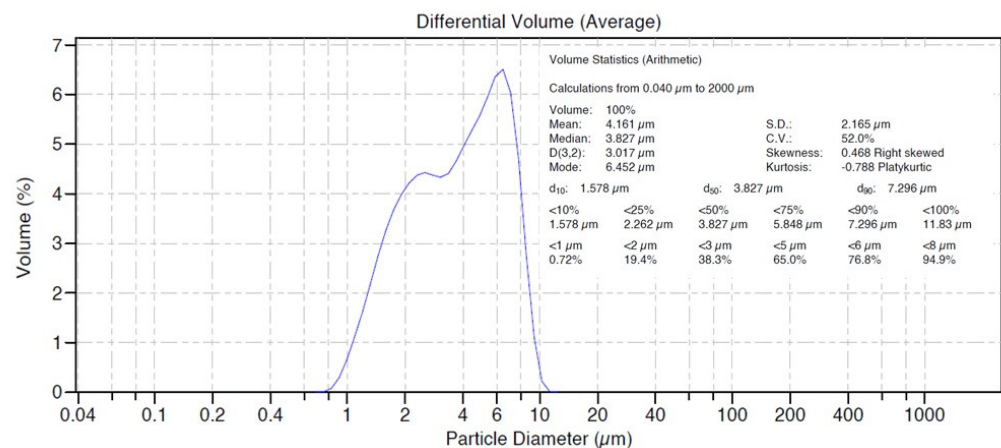


Figure 6. Particle size distribution of the solid phase of the fluorite sludge samples.

4.3. XRD

The X-ray diffractograms of the solid sludge samples shown in Figure 7 present the mineralogy of the sludge. The most abundant mineral determined via XRD in the sample from Flix is fluorite (53.1%), followed by quartz (35.6%) and untreated fluorapatite (11.3%) from the used raw material (Figure 7a), while the sample from El Hondón was mostly composed of gypsum (46.4%), followed by fluorite (40.5%), quartz (10.9%) and fluorapatite (2.3%) (Figure 7b). It is worth mentioning that the fluorite peaks are characterized by much wider shapes than the rest of the minerals. This fact could be related to the small sizes of the phases determined earlier via the particle size distribution analysis (Figure 6). Moreover, the fluorite crystals may not be accurately counted since some of these phases in the sludge could be amorphous or structurally poorly arranged. This could affect the results of the XRD; hence, the content of fluorite within the residues might be higher. The El Hondón landfill also consists of residues from other sources, which could be a reason for the elevated quantity of gypsum.

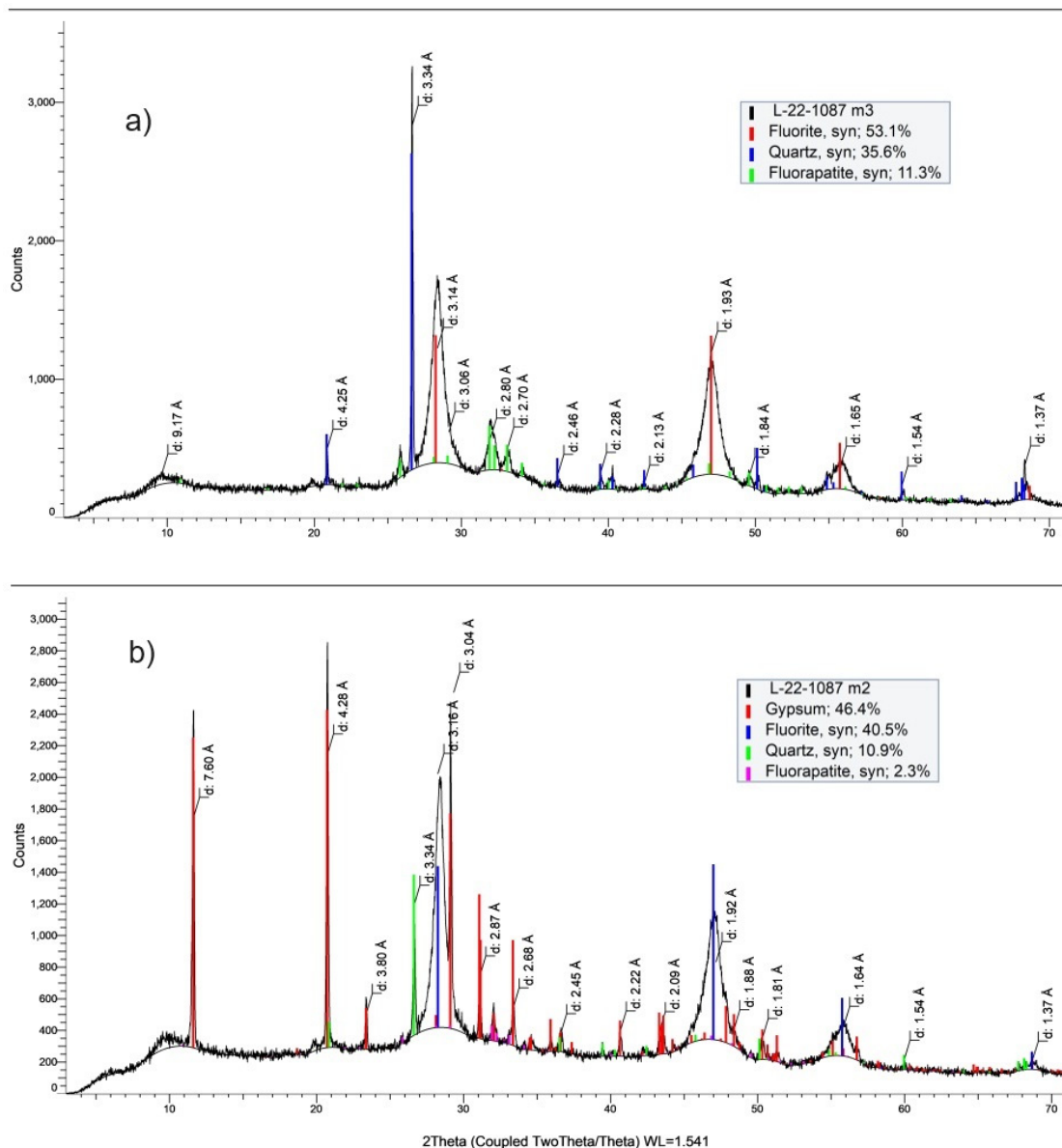


Figure 7. X-ray diffractograms of solid fluorite sludge samples from (a) Flix and (b) El Hondón.

4.4. SEM and TEM

The SEM images of the powder samples provide relevant information about the morphology and the sizes of the minerals present in the residues that can later be useful for the valorization strategies. As can be seen in Figure 8, the most abundant bright spherical particles are fluorite crystals. The other minor mineral phases found with the SEM were gypsum, quartz, iron oxyhydroxides and carbonates. Fluorite globules are present in a variety of sizes (from a few nm to a few μm) and tend to form agglomerates. Additionally, they tend to accumulate on particles of other minerals (see, for example, fluorite globules covering a crystal of gypsum on the right-hand side of Figure 8).

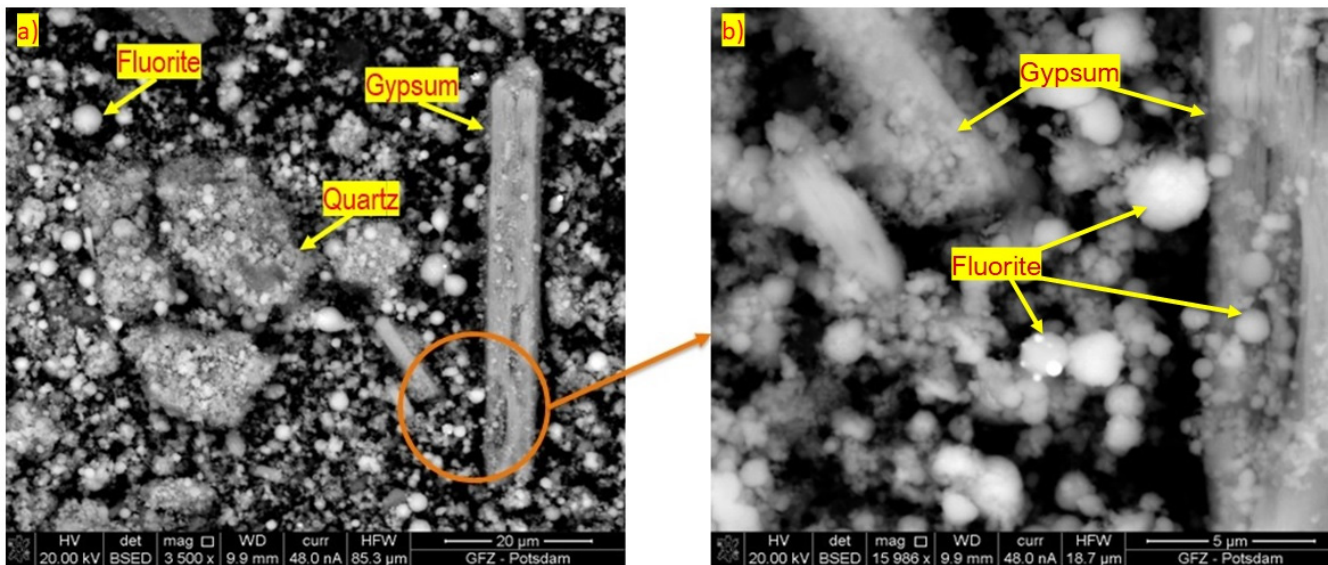


Figure 8. SEM image of the fluorite sludge sample: (a) 20 μm scale; (b) 5 μm scale (magnification).

The REEs were very difficult to detect due to their low concentrations (compared to the detection limit of the technique), and few 3d metals such as Cr, V, Ti and Mn present at the same energies as the REEs, as illustrated in the TEM image in Figure 9. The characteristic X-ray lines of these metals overlapped with the ones from the REEs. Figure 9 illustrates the STEM image as well as the experimental and modeled spectra of the investigated fluorite sludges in the region from 4 to 7 keV, which is the zone where the peaks of the REEs should be present. It can be clearly seen that the fitting looks much more accurate when the 3d metals are considered (c; red) instead of the REEs (c; grey). All of the characterized spectra were similar and did not depend on the analyzed mineral, which was most probably caused by the fluorite particles covering the other phases. The SEM and TEM analyses did not allow for the host mineral phase of the REE in the sludge to be confirmed.

4.5. μXRF

Considering that the conventional techniques did not allow for the determination of which mineral within the residues is hosting the rare earths, the samples were analyzed in a synchrotron facility using μXRF with a subsequent spectral analysis. Similar to the measurement conducted via SEM, there were difficulties with the determination of some of the REEs, mainly due to the overlapping of the characteristic X-ray lines of La and Ce with the lines of Ti and V. Additionally, the X-ray lines of Si and P (elements with very high concentrations in the samples) were superimposed with the lines of Y; therefore, yttrium, with concentrations of more than 1000 ppm in the measured samples, was not possible to detect. However, compositional maps that can be seen in Figure 10a show the presence of the Nd hot spots, associated with a phase that is rich in Ca and F, most certainly fluorite. To confirm that hypothesis, a spectral analysis of these hot spots was performed, and it is shown in Figure 10b, c. It shows a comparison of the experimental fit (acquired from

the measurement) and the theoretical one (considering the elements occurring inside of the studied sample). Figure 10b, where the Nd is not considered, clearly shows the lack of an element(s) in the zones from 5.1 to 5.3 keV and from 5.6 to 5.7 keV. Knowing that the L X-ray emission lines of Nd have energies of 5.2 and 5.7 keV, adding this element has caused both the theoretical and experimental spectra to fit much more accurately. This fact confirms the presence of Nd within the fluorite particles, supporting the hypothesis that the precipitating fluorite captures REEs during the reaction of phosphorite with HCl. The remaining REEs were not present in sufficient concentrations to be detected in the beamline or they were impossible to detect due to the overlapping of the characteristic X-ray lines with other elements. However, due to the very similar properties of all REEs, and due to the fact that they are usually found together in geologic deposits, their presence is expected inside of the calcium fluoride matrix.

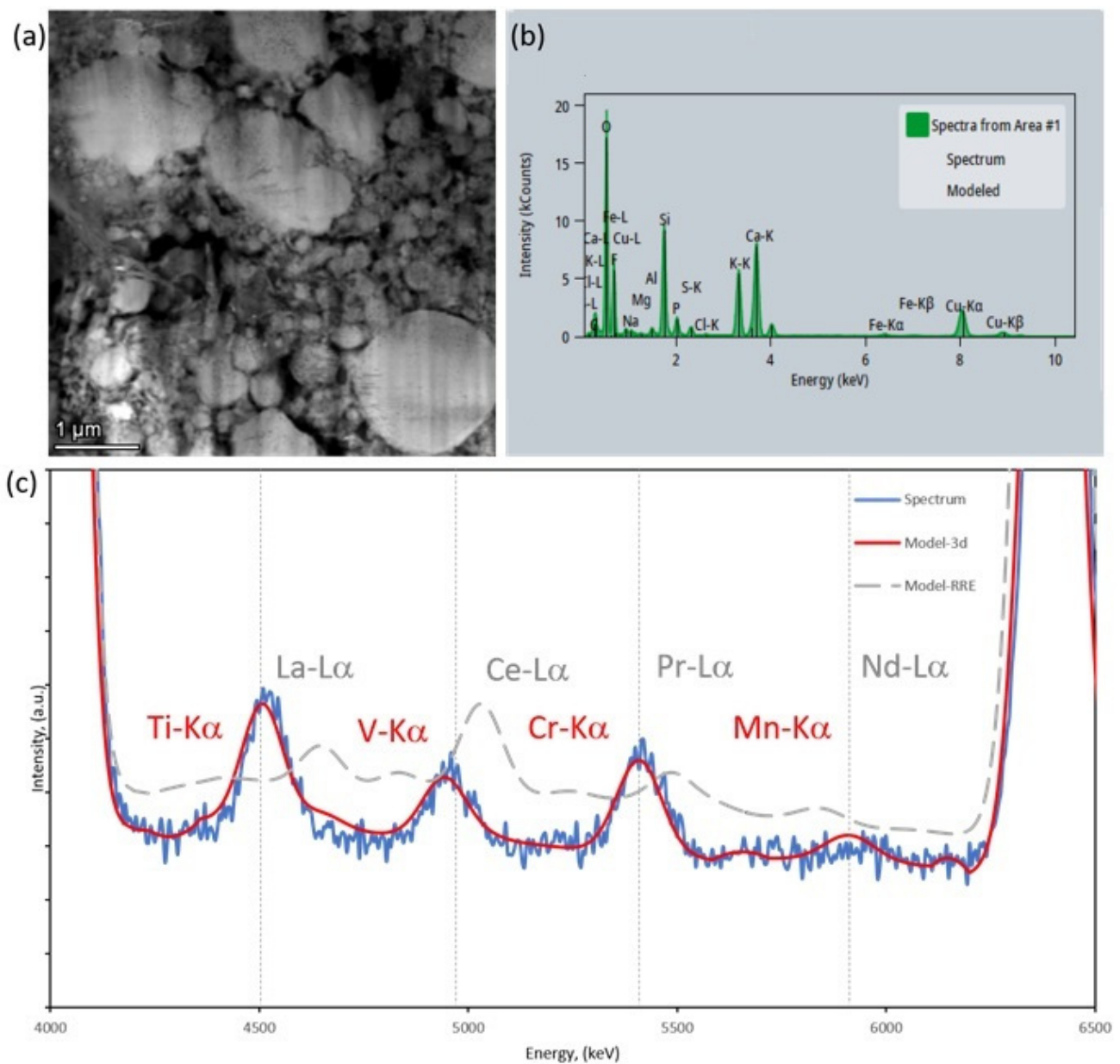


Figure 9. (a) HAADF image; (b) integrated spectrum from the area imaged in (a); (c) experimental and two simulated spectra of the region of 4 to 7 keV of the solid fluorite sludge sample with considered 3d metals (Ti, V, Cr and Mn shown as red) and REEs (dashed grey).

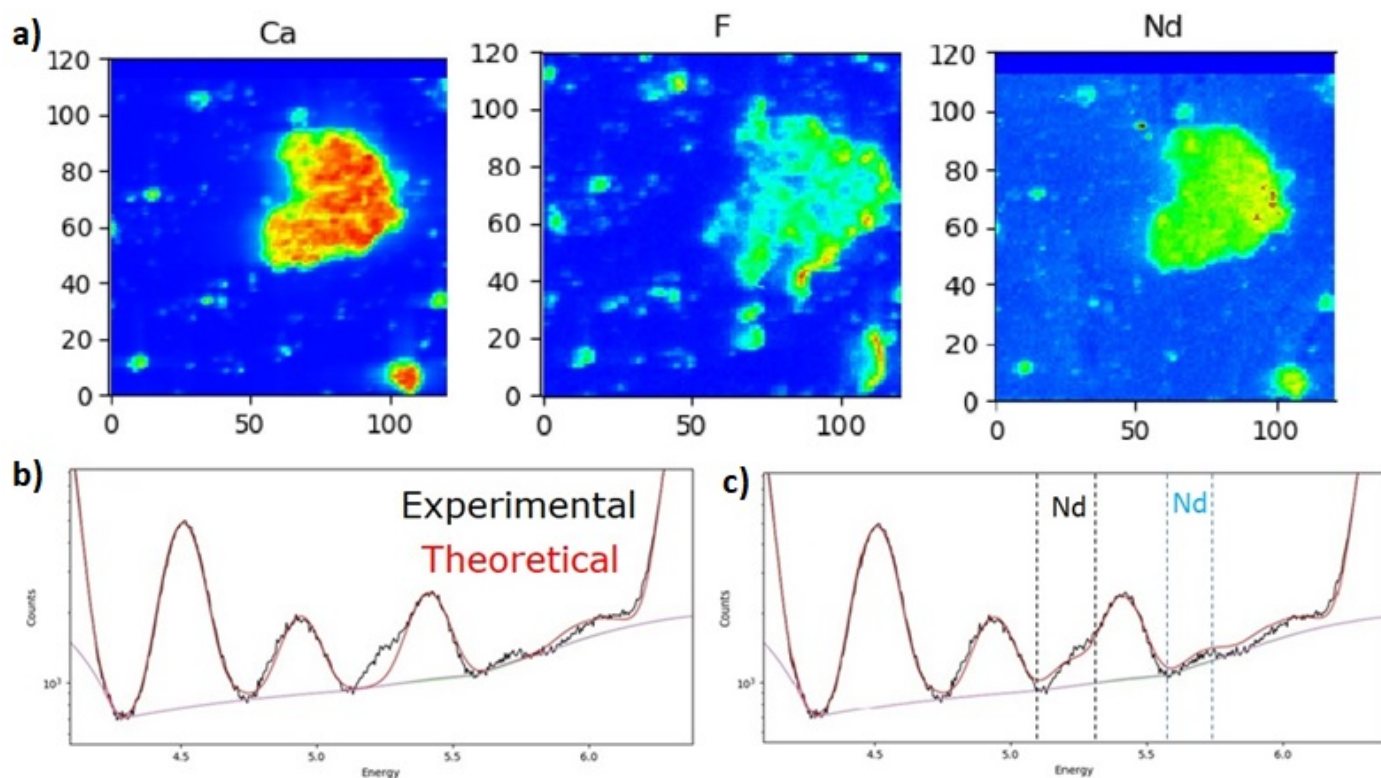


Figure 10. μ XRF analysis of the solid fluorite sludge sample. (a) Compositional maps. Red: high concentration of elements; green: low concentration of elements; blue: no elements found. (b) Fitted elemental spectra of the hot spots without Nd and (c) fitted elemental spectra of the hot spots with considered Nd.

5. Economic Assessment

Currently, the prices of raw fluorite and REEs are high with a systematic increase over the past years [7,8]. The price for a metric ton of acid grade (more than 97% CaF_2) fluorspar imported to the United States reached, in the fourth quarter of 2022, an average of USD 384, while the metallurgical grade (less than 97% CaF_2) fluorite had an average price of USD 223 [9]. The average price of fluorspar in the European market (min. 97% purity, imported from China) was, in the first half of 2023, EUR 420 per metric ton [10]. As for the REEs' high-purity oxides, the highest average prices in the past 6 months were 63 EUR/kg for Nd oxide, 5 EUR/kg for Ce oxide, 3 EUR/kg for La oxide, 260 EUR/kg for Dy oxide, 10 EUR/kg for Y oxide or 660 EUR/kg for Sc oxide [10]. Considering the concentrations of these elements that are only present in the El Hondón landfill, EUR 19 M worth of Nd and EUR 22 M worth of Dy are available to be extracted. Assuming that only 40% of the whole waste is pure CaF_2 , the value of just the fluorspar that is present in El Hondón is approx. EUR 154 M. This could create an incentive for the owners of the disposal sites to recycle the waste and find an efficient method for the separation of fluorite and/or REEs.

6. Conclusions

The characterization of fluorite sludge residue has shown potential REEs recovery from the landfills accumulated by the DCP industry considering their concentrations and the abundance of the stockpiled material. Considering the dependence of the European REEs market on external suppliers, fluorite sludge could turn out to be one of the sources to contribute to the domestic production of these critical raw materials. According to the analysis performed in this study, the sludges consist mostly of fluorite, which is another critical material that could be supplied if a sufficiently effective separation technique of this mineral was developed. The initial stages of this process were already studied,

yet successful tests to obtain a high enough purity for the market are still pending to be accomplished. The separation of some parts of the waste would be beneficial for all parts since the site owners could resell a significant part of the accumulated material with a simultaneous reduction in the landfilled volume, hence diminishing the impacts of the residues on the surroundings. Moreover, fluorite sludge could be treated directly in the decantation stages in the factories instead of landfilling it, obtaining higher REEs concentrations and a higher extraction efficiency.

The first step in the purification of the residues would be the removal of the radionuclides that are present within them for the safe and secure extraction of fluorite or rare earths without radiological protection actions. Preliminary tests have already been performed, but bigger scale experiments still must be undertaken for efficient commercial extraction. The separation of uranium and radium from the residue will allow for the reduction in the environmental impacts of the landfills and facilitate the recycling option, contributing to the circular economy model.

Author Contributions: Conceptualization, M.P. and F.G.; methodology, F.G.; validation, F.G.; formal analysis, M.P. and F.G.; investigation, M.P., F.G., V.R. and M.D.S.; writing—original draft preparation, M.P.; writing—review and editing, F.G.; supervision, F.G.; project administration, F.G. All authors have read and agreed to the published version of the manuscript.

Funding: This research received funding from the European Union’s Horizon 2020 research and innovation program under the Marie Skłodowska-Curie Grant Agreement No. 857989 (ITN-Panorama Project) and the European Union’s Horizon 2020 research and innovation programme under grant agreement no. 101005611 for Transnational Access conducted at Helmholtz-Zentrum Potsdam Deutsches Geoforschungszentrum (GFZ). Finally, this study was partially funded by the Catalan Agency for Business Competitiveness (ACCIO) through Project Terrari (RDECR19-1-0013).

Institutional Review Board Statement: Not applicable.

Informed Consent Statement: Not applicable.

Data Availability Statement: Not applicable.

Acknowledgments: The authors thank the European Regional Development Fund and the State of Brandenburg for the Themis Z TEM (part of the Potsdam Imaging and Spectral Analysis Facility (PISA)). We acknowledge SOLEIL for the provision of synchrotron radiation facilities and we would like to thank Delphine Vantelon and Camille Rivard for their assistance in using the beamline “LUCIA” under proposal number 20211173. Also, we thank Frederic Clarens and Albert Martínez from Eurecat for their help in the sludge characterization.

Conflicts of Interest: The authors declare no conflict of interest.

References

1. Arruda-Neto, J.D.T.; Tavares, M.V.; Filadelfo, M. Concentrations of uranium in animal feed supplements: Measurements and dose estimates. *J. Radioanal. Nucl. Chem.* **1997**, *221*, 97–104. [[CrossRef](#)]
2. Mola, M.; Palomo, M.; Peñalver, A.; Aguilar, C.; Borrull, F. Distribution of naturally occurring radioactive materials in sediments from the Ebro river reservoir in Flix (Southern Catalonia, Spain). *J. Hazard. Mater.* **2011**, *198*, 57–64. [[CrossRef](#)]
3. Cánovas, C.R.; Macías, F.; Pérez-López, R.; Nieto, J.M. Mobility of rare earth elements, yttrium and scandium from a phosphogypsum stack: Environmental and economic implications. *Sci. Total Environ.* **2018**, *618*, 847–857. [[CrossRef](#)] [[PubMed](#)]
4. Casacuberta, N.; Masqué, P.; García-Orellana, J. Fluxes of ²³⁸U decay series radionuclides in a dicalcium phosphate industrial plant. *J. Hazard. Mater.* **2011**, *190*, 245–252. [[CrossRef](#)] [[PubMed](#)]
5. García-Talavera, M.; Matarranz, J.L.M.; Salas, R.; Ramos, L. A regulatory perspective on the radiological impact of NORM industries: The case of the Spanish phosphate industry. *J. Environ. Radioact.* **2011**, *102*, 1–7. [[CrossRef](#)] [[PubMed](#)]
6. Solé, V.; Papillon, E.; Cotte, M.; Walter, P.; Susini, J. A Multiplatform Code for the Analysis of Energy-Dispersive X-ray Fluorescence Spectra. *Spectrochim. Acta Part B At. Spectrosc.* **2006**, *62*, 63–68. [[CrossRef](#)]
7. Statista. Fluorspar Price in the United States from 2014 to 2022. Available online: <https://www.statista.com/statistics/1051742/fluorspar-price-us/> (accessed on 27 June 2023).
8. Statista. Average Price of Selected Rare Earth Oxides from 2015 to 2022. Available online: <https://www.statista.com/statistics/617249/price-range-of-selected-rare-earth-oxides/> (accessed on 27 June 2023).

9. USGS. *Fluorspar in the Fourth Quarter 2022. Mineral Industry Surveys*; USGS: Reston, VA, USA, 2022.
10. Institut für Seltene Erden und Strategische Metalle AG. Metal Prices. 2023. Available online: <https://institut-seltene-erden.de/> (accessed on 13 June 2023).

Disclaimer/Publisher's Note: The statements, opinions and data contained in all publications are solely those of the individual author(s) and contributor(s) and not of MDPI and/or the editor(s). MDPI and/or the editor(s) disclaim responsibility for any injury to people or property resulting from any ideas, methods, instructions or products referred to in the content.